Computational Fluid dynamics simulations on Drag-based wind turbine design for higher energy capture

Abderahmane Marouf, PhD, Doctor of Engineering (DEng), Computational Fluid Dynamics , École Normale Supérieure de Paris, France, Master's degree, Computational Engineering – Mechanicals, University of Strasbourg, Germany

CONTENT

CHAPTER 1

Introduction

The issue of electrical energy takes precedence among governments, companies, and research institutions in addition to CO2 and climate change. A continuous influx of perspectives revolves around the optimal selection of generation technologies, a matter of interest for both developed and developing nations. The confluence of decreasing fossil-fuel reserves, stricter environmental mandates, and the insatiable appetite for energy has steered the trajectory towards alternative renewable energy solutions.

Among these alternatives, ***wind energy*** *known as* ***a green energy*** emerges as a frontrunner due to its remarkable growth and potential. Wind power exhibits the second-highest growth rate among renewable energy sources, with a recent annual expansion rate of approximately 34% (according to (Bazmi AA, 2011). A comprehensive evaluation of sustainability indicators in 2009 has established wind power as an environmentally favorable option compared to hydropower, photovoltaic, and geothermal energy, exhibiting lower greenhouse gas emissions, minimal water consumption, and more favorable social impacts (Annette Evans, 2009).

Anticipated Progress:

Projections indicate that by 2030, a substantial proportion – at least 20% – of the energy demand in the United States will be met by onshore and offshore wind farms (Lindenberg S, 2008). To achieve this ambitious target within the next 15 years, a dual-pronged approach is required: a significant augmentation in wind turbine installations across onshore and offshore farms and an enhancement in turbine operability. Moreover, this must be achieved while ensuring economic viability and competitive energy costs (Lindenberg S, 2008).

Technical Advancements and Challenges:

The pursuit of economical energy production has driven the enlargement of commercial wind turbines over the past three decades. This strategic upscaling is financially advantageous due to the principle that increased hub-height and rotor radius correspond to higher captured wind speeds. Consequently, fewer turbine units are necessary to achieve desired power outputs in wind farms, resulting in reduced operational expenditures. However, the scaling-up presents concurrent challenges in terms of structural integrity and durability. The optimal rotor diameter attainable with current materials and manufacturing techniques remains an ongoing concern. Furthermore, alongside technical demands, wind turbines must conform to evolving energy policies, international agreements, and governmental regulations (R. Saidur, 2010) .

Optimization Imperative:

Wind turbine design inherently embodies an optimization paradigm, wherein optimal solutions are sought within defined design constraints and specific objectives. Diverse objectives, constraints, algorithms, tools, and models have been proposed by researchers to optimize wind turbine performance. The escalating interest in this field is evident from the exponential growth in research publications catalogued in the Scopus database. While some researchers have examined the impact of varying optimization objectives on solution quality, others have assessed optimization algorithms, energy policies, economic implications, and environmental repercussions. Many scholars have introduced diverse optimization methodologies and strategies.

Future innovative designs

The optimization of horizontal wind turbines presents a dynamic and multifaceted research area, characterized by diverse objectives, constraints, and resolution strategies. As the world steers toward renewable energy solutions, the confluence of scientific insights, innovative methodologies, and engineering process holds the potential to reshape the landscape of wind energy conversion, rendering it more efficient, sustainable, and impactful. Aerodynamic forces acting on the turbine include drag and lift forces. A drag-based turbine uses drag forces as the primary force for energy conversion, making it the main driving force. The company Xenecore[1] proposes an

innovative wind turbine design that utilizes optimized fan-shaped blades. These lightweight fan-shaped blades have a larger area, nearly 17 times that of conventional wind turbine blades. This significant increase in blade area leads to a considerable enhancement of the drag force, resulting in more effective energy conversion.

Experimental tests aimed at optimizing drag-based turbines and quantifying the energy conversion from the wind are both expensive and time-consuming. The potential for employing computational fluid dynamics (CFD) in the design process for these new configurations is emphasized in this study. Two turbines are examined using a theoretical approach involving an internal tunnel disc actuator, which seeks to achieve maximum drag and evaluate the power generated by these drag-based turbines. Methodology.

Comparative analysis of wind, hydro, and solar Energy sources

Solar energy, harnessed through photovoltaic (PV) systems, has a variability in generated power based on photovoltaic panel efficiency, geographic location and weather conditions. The average generated power by solar panels can achieve 150 to 250 watts per square meter in standard conditions. However, high initial cost for solar panels needs to be taken into account and requires good solar exposure. Hydro-electric power generation depends on the flow rate and the vertical distance over which the water falls. For a head of 1 meter and flow rate of 1 cubic meter per second, hydroelectric system can yield approximately 981 watts per square meter of water cross-sectional area. The hydropower is not suitable in many areas due to lack of resources, requires substantial modification of water resources, and installation cost could be high.

The energy we can convert from the wind per square meter is impressive. A space of 200 meters in length and 15 meters in width, totaling 3000 square meters. This area could generate a remarkable 3 gigawatts, equal to 1 megawatt per square meter. In contrast, solar energy, limited to one level, produces only around 200 watts. Wind power's potential is over two million times greater than solar power per square meter. Moreover, wind power isn't confined to the ground; it can go upwards with 500 levels, making use of the sky's vast potential. This flexibility is key to fighting the fast pace of climate change. It's clear that wind energy is our best bet against this urgent challenge.

The Altaeros Energies has created the Buoyant Air Turbine (BAT), which uses an inflatable shell to float for thousands of feet above the ground. This higher position allows it to capture speed winds that are five to eight times stronger and more dependable than those closer to the ground where traditional turbines are located. At an altitude of 150,000 feet, wind speeds reach a remarkable 300 mph. This substantial increase in wind velocity could potentially amplify the previously mentioned 3 gigawatts to 9 times its value, resulting in 27 gigawatts of energy output. Theoretically, this amounts to a staggering 20 million times the power generated by solar energy. Moreover, when considering the entirety of the sky's circumference, this potential amplification factor extends further

Numerical methodology

2.1. Actuator Disc Model:

The calculation is based on the kinetic energy of the wind as it traverses through an actuator disk or a hypothetical model illustrating ideal turbine blades, as depicted in Figure 1. In this context, the efficiency's maximum value is redefined. Several crucial parameters are defined, including the far-field pressure (P_{stream}), as well as $P1$, $V1, P2,$ and $V2$, representing the pressures and velocities under upstream (inflow) conditions and downstream (outflow) conditions of the turbine.

The velocity V_t is the speed crossing the turbine blades.

The mass flow conservation inside the tunnel can be written in 3 different positions as follows:

$$V_1 A_1 = V_t A_t = V_2 A_2$$

The force on the turbine results in change in momentum:

$$F = \dot{m} . \Delta v$$

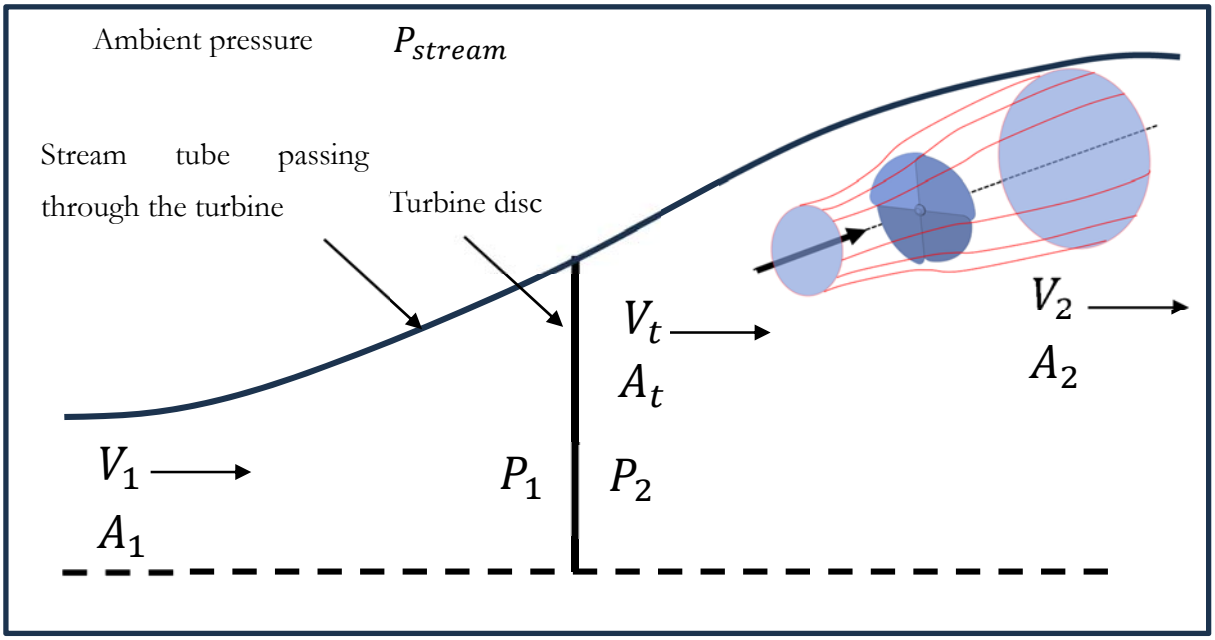

Figure 1: Schematic description of the disc actuator model

The sudden change in the air flow velocity impacting the turbine disc exerts a change in momentum. The force can be computed by multiplying the mass flow rate $\dot{m}$ by the change in the velocity Δv. The force can be articulated in relation to the designated variables (illustrated in figure 1) as presented below:

$$(P1 - P2)A_t = \rho A_1 V_1 (V_1 - V_2)$$

Wind energy converters employ aerodynamic drag are based on the difference between both velocity speeds $(V_1 - V_2)$. In contrast to other wind turbines that rely on lift, the suggested wind turbine utilized drag force for energy conversion. The power extraction P, can be computed using the aerodynamic drag D, the area A and the velocity V1 at which it operates is expressed as P = D. V1. The resultant Drag is expressed as follows:

$$D = \frac{\rho}{2} C_D (V1 - V2)^2 A$$

In order to achieve maximum power output, it becomes essential to optimize the drag force to effectively convert the entire energy within the airflow. This necessitates the maximization of the difference between V1 and V2 velocities.

2.2. Numerical model:

Two distinct types of turbine blades have been chosen for the purpose of conducting computational fluid dynamics (CFD) simulations. The first prototype compromises 30 blades, all assembled together and set at a 45 degrees, as illustrated in figure 2. The second prototype presented in figures 3, contains 4 blades. Both sets of turbine blades are placed inside the actuator disc model tunnel. The blades radius is fixed at 100 meters in order to simulate real-world wind conditions.

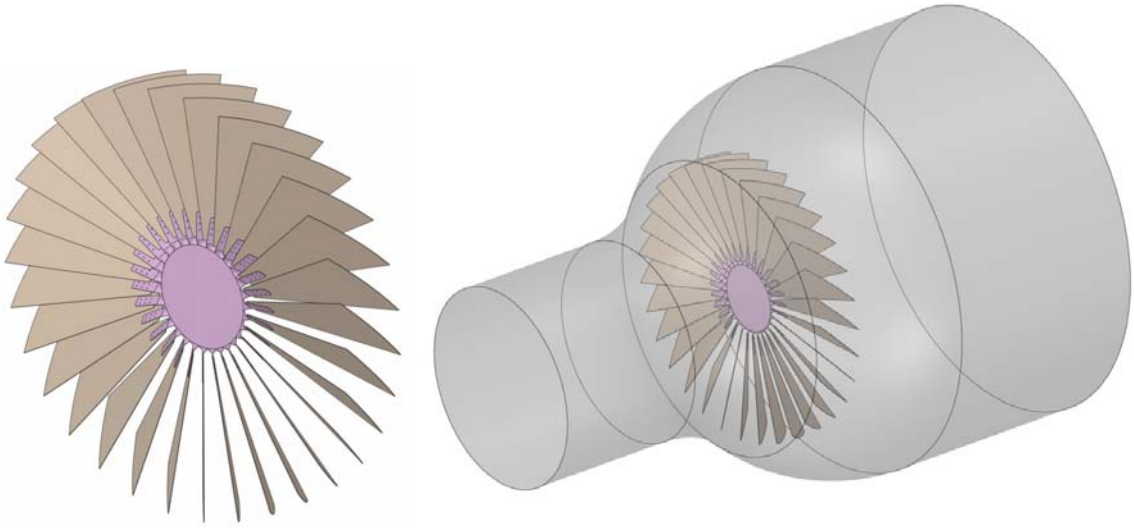

Figure 2: CAD design of the 30 blades inside the tunnel

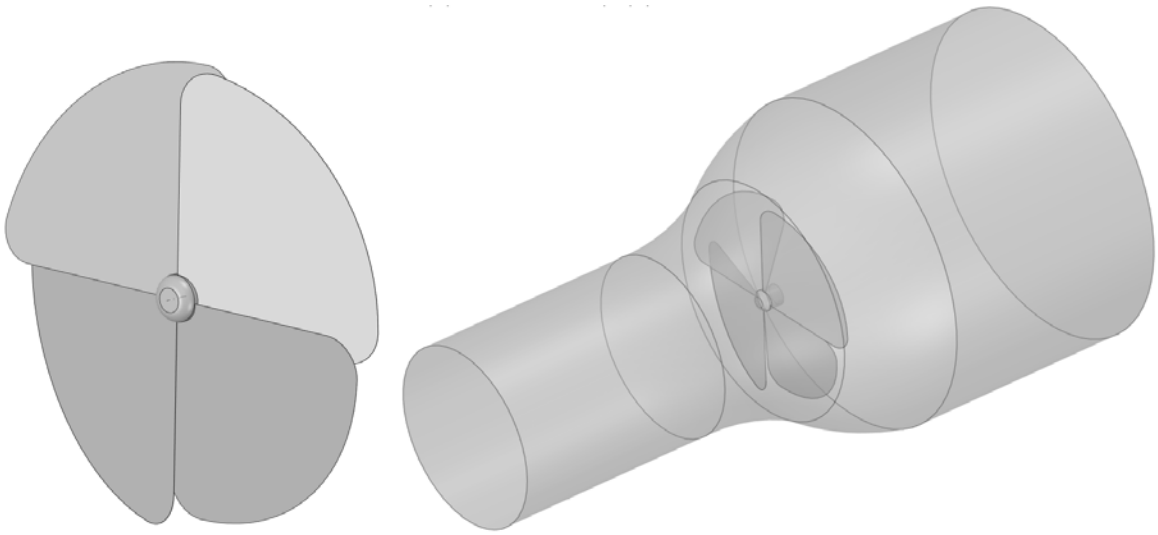

Figure 3: CAD design of the 4 blades inside the tunnel

Computational Fluid Dynamics is an established simulation methodology and technique employed to simulate fluid flow behaviors. In Autodesk CFD, the Finite Element method (FEM) is employed. The application of CFD analysis extends to the examination of the entire tunnel containing the turbine blades within it. This approach aids in identifying the trajectory of airflow and resultant forces acting upon the turbine blades, consequently determining the energy output of the system. Furthermore, the potential to include blade rotation enables the calculation of generated power.

The software generates the mesh automatically using unstructured elements. Both configurations contain several millions (1 to 3) of fluid elements, nodes and cells, wherein the flow characteristics (velocity, pressure, etc.) are calculated. Concerning the boundary conditions, the tunnel consists of an inlet denoted by the small circle surface on the left (as shown in figures 2 and 3). The outlet is represented by a larger circular surface, while the tunnel's surfaces are treated as walls, including the turbine blades. The velocity is set at 100 mph (44.7 m/s), and the outlet is maintained at free pressure condition, facilitating the fluid's exit from the tunnel and preventing reverse flows.

Results

In the present investigation, computational studies have been undertaken to explore the influence of flow forces on the blades free rotation. Dynamic have been conducted at the rotational speed of the blades. Figures 4 and 5 highlight the flow trajectory around both configurations of turbine blades. The red-colored surface on both turbines indicates the presence of a high static pressure field exerted by the flow on the blades. Specifically, this pressure reaches 3.9 kPa for the configuration with 30 blades and 1.46 kPa for the one with 4 blades, both under identical flow conditions. The outcomes demonstrate that the setup featuring 30 blades can yield a more extensive pressure distribution. By integrating pressure across the area, the total force capable of being converted into energy is obtained.

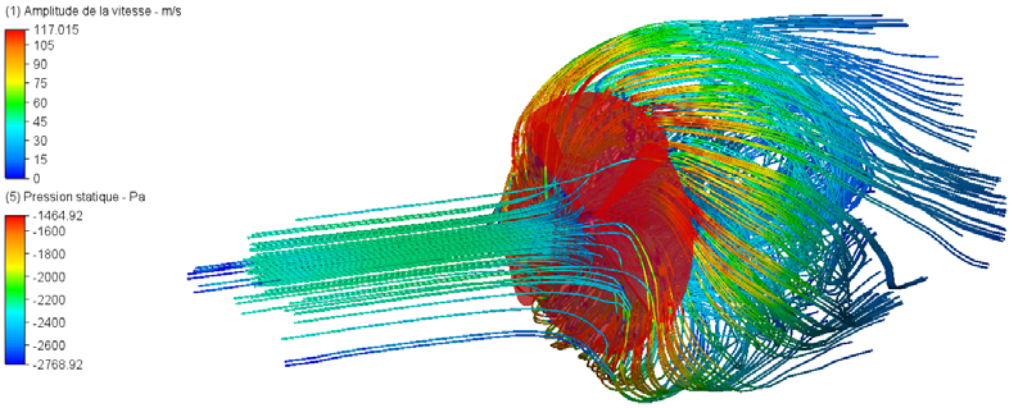

Figure 4 : Streamlines colored by the velocity magnitude and surface pressure around the 4 blades turbine.

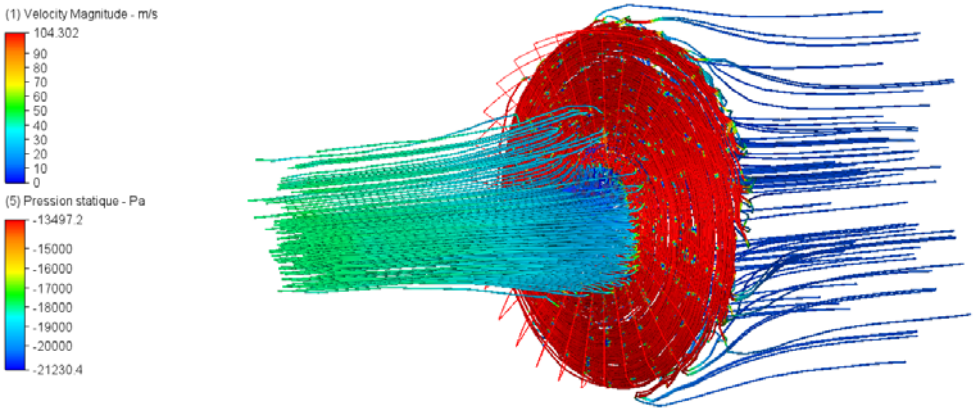

Figure 5 : Streamlines colored by the velocity magnitude and surface pressure around the 4 blades turbine.

Figure 6 illustrates the sectional planes along both the streamflow and transverse directions for both configurations. It is evident that both turbines, when subjected to aerodynamic forces, exhibit a notable increase in rotational velocity.

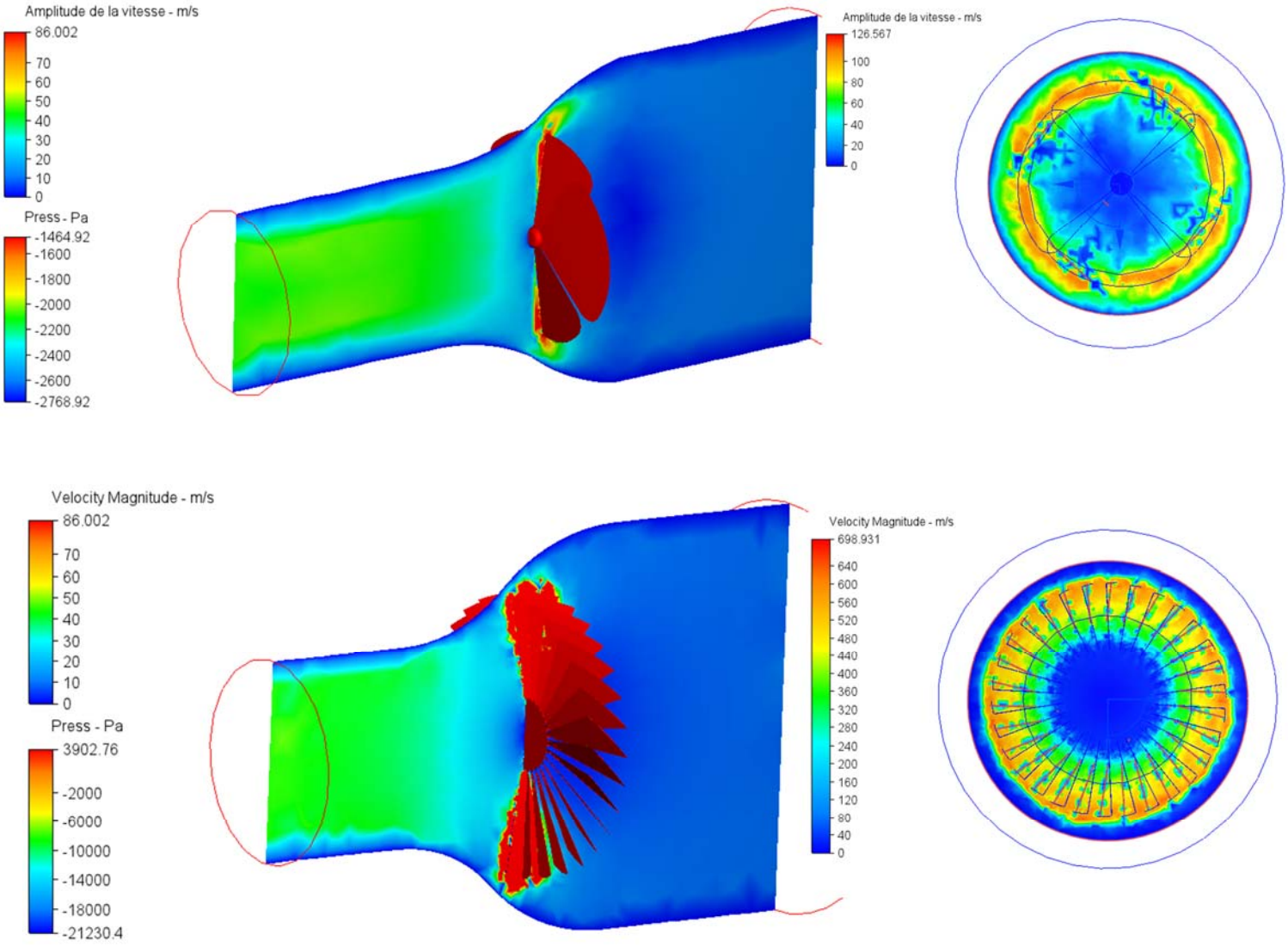

Figure 6 : Velocity magnitude extracted from streamflow and crossflow plane around the 4 and 30 turbine blades.

The pressure field for the wind turbine is illustrated in Figure 7. It reveals a region of high pressure situated upstream of the turbine with 4 blades, transitioning to a lower pressure immediately behind it.

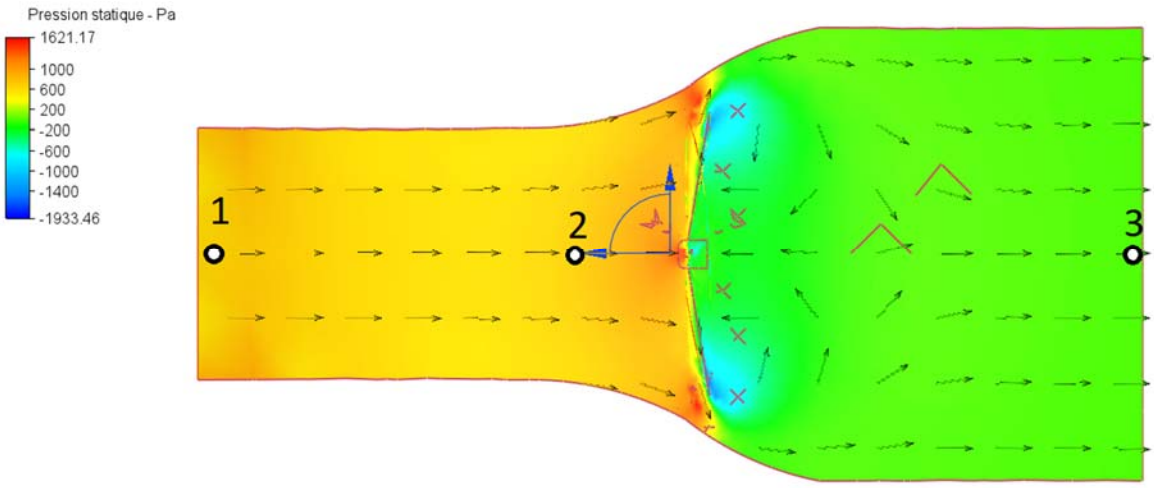

Figure 7: Pressure field in the tunnel of 4 blades configuration and the 3 selected monitor points to extract velocity.

3 monitoring points have been extracted from the flow field, as presented in Figure 7, to illustrate the temporal variations in velocity magnitude. The velocity ultimately converges at 100 mph (44.7 m/s) as shown in figure 8.

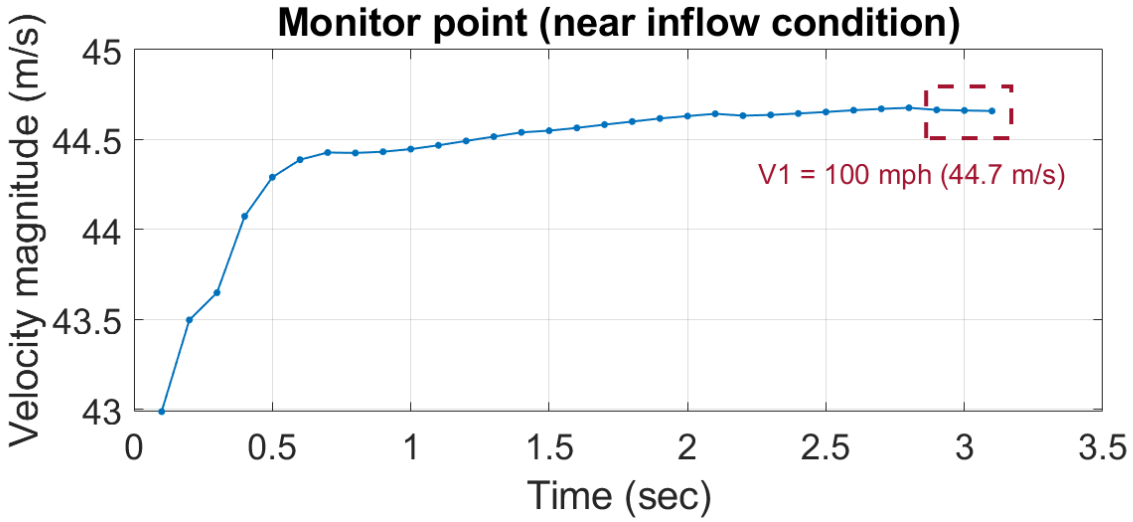

Figure 8: Velocity magnitude as a function of time of simulation for a monitor point near inlet boundary condition.

The second monitoring point has been selected near of the outlet region, as indicated in Figure 9.

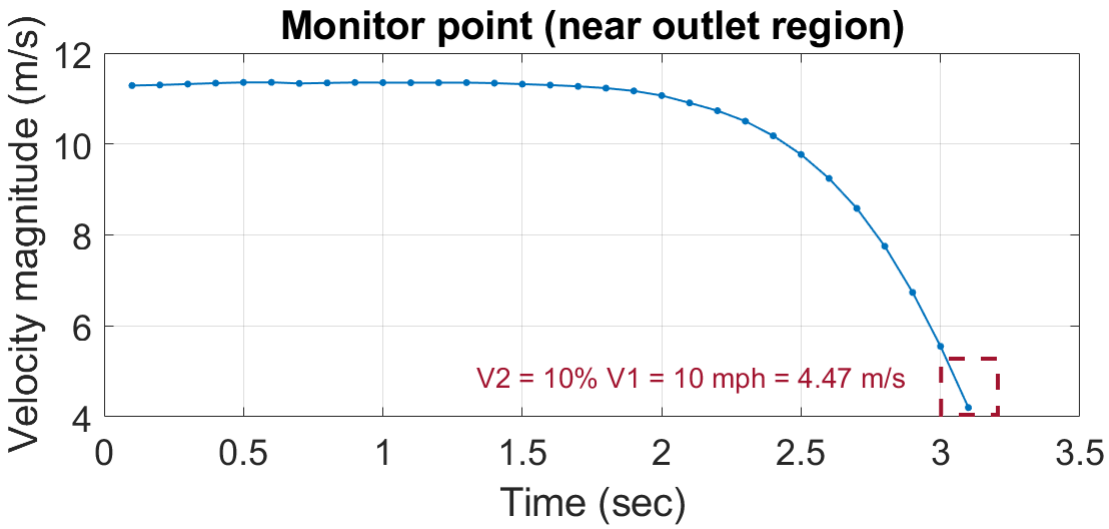

Figure 9: Velocity magnitude as a function of time of simulation for a monitor point near inlet boundary condition.

After the simulation converges, the velocity stabilizes at 10 mph (4.47 m/s), constituting 10% of the inflow velocity, V1. The significant difference between V1 and V2 contributes to generating a maximum drag force. Consequently, this type of drag-based turbine blades has the potential to convert a maximal amount of energy..

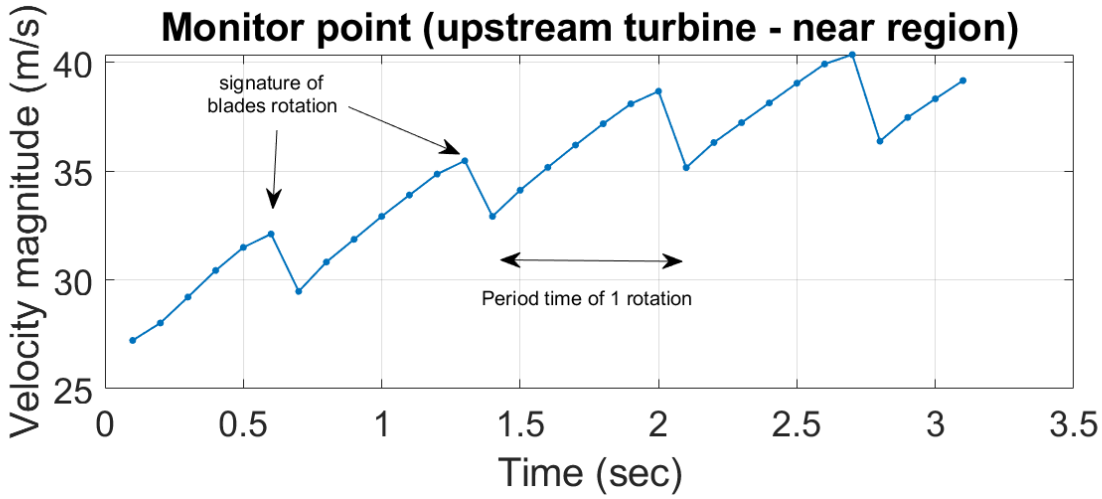

Figure 10: Velocity magnitude as a function of time of simulation for a monitor point upstream turbine boundary condition.

Additionally, a monitoring point upstream of the turbine has been extracted (as depicted in Figure 10) to ascertain the suitable revolutions per minute (RPM) of the blades by analyzing their impact on the flow. As illustrated in Figure 10, repetitive peaks coincide with the blade rotation. The rotational period, denoted as T, measures 0.75 seconds, yielding an airflow-induced rotation of 80 RPM for the 4-blade turbine. Conversely, the 30-blade configuration displays elevated surface pressure, contributing to a calculated RPM of 95, similarly demonstrated in the earlier figures.

- **Calculation of the generated power:**

To compute the converted power from the drag force, two methodologies can be employed. The first approach involves establishing a correlation between power and airflow properties, such as:

$$P_m = \frac{1}{2}\,\rho A\, V_0^3 C_p = \frac{1}{2}\,.1.2\,.(\pi\,.100^2)(44.7)^3\,.0.5 \approx 1\ Gwatt.$$

In this equation, ρ represents air density, A stands for the total area of the turbine, V_0 signifies the streamflow velocity, and C_p represents the effective pressure coefficient. Nevertheless, this is a simplified methodology that does not take into account the rotation of blades.

The second methodology is founded from the pressure distribution acquired from the surfaces of the wind blades and their corresponding areas. Subsequently, the power is computed using the force and velocity.

Table 1: Illustration of the surface area and the pressure distribution for each blade (4 blades turbine)

Blades N° =>	1	2	3	4
Surface Area for each blade (m^2)	8.37387e+03	8.37387e+03	8.37387e+03	8.37387e+03
Pressure (Pa)	254.127	367.51	318.025	344.887
Total drag forces N	1,08E+07 N			

The generated power is then calculated by using the drag force from table 1:

$$P = D \,.V$$

$$\boldsymbol{P = \ 1.08E + 09\ watt = 1.08\ G\ watt}$$

Table 2: Illustration of the surface area and the pressure distribution for each blade (30 blades turbine)

Blades N° =>	1	2	3	4	5	6	7	8	9	10
Surface Area (m^2)	3600	3600	3600	3600	3600	3600	3600	3600	3600	3600
Pressure (Pa)	251.497	298.165	308.083	275.048	385.096	326.616	313.356	258.441	219.384	256.548
	11	12	13	14	15	16	17	18	19	20
Surface Area for each blade (m^2)	3600	3600	3600	3600	3600	3600	3600	3600	3600	3600
Pressure (Pa)	319.985	286.565	319.488	302.646	442.014	145.704	555.705	157.816	107.235	351.258
	21	22	23	24	25	26	27	28	29	30
Surface Area for each blade (m^2)	3600	3600	3600	3600	3600	3600	3600	3600	3600	3600
Pressure (Pa)	222.497	334.441	221.406	219.995	121.986	247.958	304.936	377.608	163.85	126.897
Total drag force	2,97E+07 N									

The generated power by the 30 blades is then calculated by using the drag force from table 2:

$$\boldsymbol{P = D\,.V}$$

$$\boldsymbol{P = \ 2.97E+09\ watt = 2.97\ G\ watt}$$

Conclusion

This study presents a numerical investigation into the utilization of drag-based wind turbines using theoretical conditions within a disc actuator tunnel model. Two distinct configurations have been analyzed: one with 4 blades and another with 30 blades, both positioned within the tunnel. The blades possess a radius of 100 meters, and the inflow velocity is set at 100 m/s (44.7 mph). Computational fluid dynamics (CFD) modeling has been employed to compute the velocity fields and pressure distribution along the turbine blades. The blades are allowed to rotate freely due to the force exerted by the airflow, resulting in a significant degree of rotation. Consequently, the power generated from the 4-blade turbine amounts to 1.08 GW, while the 30-blade configuration yields 2.97 GW.

References

Annette Evans, V. S. (2009). Assessment of sustainability indicators for renewable energy technologies. *Renewable and Sustainable Energy Reviews*, Volume 13, Issue 5, Pages 1082-1088.

Bazmi AA, Z. G. (2011). Sustainable energy systems: Role of optimization modeling techniques in power generation and supply—A review. *Renewable and Sustainable Energy Reviews*, Volume 15, Issue 8, Pages 3480-3500.

Lindenberg S, S. B. (2008). wind energy by 2030. . *National renewable energy laboratory (NREL), US department of energy, renewable energy consulting services, energetics incorporated*.

R. Saidur, M. I. (2010). A review on global wind energy policy. *Renewable and Sustainable Energy Reviews*, Pages 1744-1762.